Available online at www.sciencedirect.com
SCIENCE DIRECT®
Surface Science 577 (2005) L78–L84
SURFACE SCIENCE
www.elsevier.com/locate/susc

Surface Science Letters

h-BN on Pd(1 1 0): a tunable system for self-assembled nanostructures?

Martina Corso *, Thomas Greber [1], Jürg Osterwalder [2]

Physik Institut, Universität Zürich, Winterthurerstrasse 190, CH-8057, Zürich, Switzerland

Received 14 October 2004; accepted for publication 12 January 2005
Available online 22 January 2005

Abstract

A one-monolayer thick covalent network of hexagonal boron nitride (*h*-BN) forms on Pd(1 1 0) upon thermal decomposition of borazine $(HBNH)_3$. Due to the weak interfacial bonding, the different symmetries of overlayer and substrate, and the lattice mismatch, a variety of rotated domains are created. Several Moiré patterns appear in STM images, which can be well explained by simple atomic models. Rings in LEED manifest domain averaging. Non-uniform intensity distributions along these rings measure the abundance of certain domains, depending on particular preparation procedures. The individual Moiré domains represent interesting periodic nanostructures that can be imprinted in an adsorbed layer of C_{60} molecules.

Keywords: Hexagonal boron nitride (*h*-BN); Palladium; Moiré pattern; Scanning tunneling microscopy (STM); Low energy electron diffraction (LEED)

1. Introduction

Ultra-thin insulating films weakly bonded to flat metal surfaces may offer interesting applications in the construction of future microelectronic devices due to the abrupt change of the electronic structure at the interface. In the search of materials with these properties, hexagonal boron nitride (*h*-BN) has proven to be an excellent candidate. *h*-BN monolayer films were produced on a variety of transition metal surfaces, in most cases with a hexagonal symmetry [1–5] or in one case on a square lattice (Ni(1 0 0) [6]). The layers are weakly interacting with the metal but they are stable at high temperatures (up to 1000 K) and to air exposure. These important features are due to the

* Corresponding author. Tel.: +41446356697; fax: +41446355704.
E-mail addresses: corsomar@physik.unizh.ch (M. Corso), greber@physik.unizh.ch (T. Greber), osterwal@physik.inizh.ch (J. Osterwalder).
[1] Tel.: +41446355744; fax: +41446355704.
[2] Tel.: +41446355827; fax: +41446355704.

0039-6028/$ - see front matter
doi:10.1016/j.susc.2005.01.015

strong lateral inter-atomic bonds within the *h*-BN layers. The strength of these bonds plays a key role in the process of formation of *h*-BN layers on different metal surfaces, but the geometry and the lattice constant of the substrate make every system unique. In the case of *h*-BN films on Rh(1 1 1), for example, the large tensile lattice mismatch of −6.7% between the overlayer and the substrate leads to the formation of a bilayer nanomesh with a periodicity of 32 ± 2 Å [5]. Two monolayer meshes of *h*-BN with a hole diameter of 24 ± 2 Å and a wire thickness of 9 ± 2 Å grow one on top of the other, shifted such as to cover most of the substrate surface. In contrast, when *h*-BN is grown on Ni(1 1 1), the small compressive lattice mismatch of +0.4% between the two systems leads to the formation of a (1 × 1) commensurate single atomic layer. Ordered and flat terraces of one monolayer thickness are found over large areas [7,8].

In this paper we report on the rich and peculiar structural elements found when *h*-BN is formed on the (1 1 0) surface of a palladium single crystal, which does not match the hexagonal symmetry of a *h*-BN layer. Scanning tunneling microscopy (STM) and low-energy electron diffraction (LEED) measurements illustrate that the *h*-BN units do not find a unique way to register with the Pd(1 1 0) surface. A large variety of domains is formed in which the *h*-BN unit cells assume different orientations with respect to the substrate crystallographic directions while preserving their original inter-atomic distances. The weaker bonding to the substrate manifests itself by producing, for each domain, a characteristic Moiré pattern resulting from the superposition of substrate and film periodicities. A number of regular nanostructures is thus formed, with different periodicities and symmetries. There are indications that the domain distribution depends on details of the sample preparation.

2. Experimental

The experiments were performed in three ultra-high vacuum (UHV) chambers (base pressure $<10^{-10}$ Torr) connected through a low vibrational noise coupling. In this way the same sample can be transferred under UHV conditions between the LEED chamber, the STM chamber (which hosts a Park Scientific Instruments VPII STM) and the photoemission chamber (with a modified VG ESCALAB 220 spectrometer) [9,10]. STM images were recorded in constant current mode. NaOH etched W tips were used. All the data were taken on the same Pd(1 1 0) single crystal at room temperature. It was prepared by repeated cycles of Ar^+ ion bombardment (750 eV), exposure to 10 L (1 Langmuir = 10^{-6} Torr × s) of O_2 while keeping it at 750 K, and subsequent annealing to 1000 K. The *h*-BN monolayers were obtained by exposing the clean and hot (1000 K) Pd(1 1 0) surface to a borazine $(HBNH)_3$ vapor with a pressure reading of 2.3×10^{-6} Torr for 40 s (90 L). The B and N coverages were quantified by means of STM and X-ray photoelectron spectroscopy (XPS), and the cleanliness of the sample was checked with XPS (less than 1% carbon contamination was found).

3. Results and discussion

The STM pictures of *h*-BN/Pd(1 1 0) (as e.g. those in Figs. 1a and 2a) show various Moiré patterns that arise from the incommensurate growth. The domains extend up to 100 nm regardless of the presence of steps (Fig. 1a). On the other end, two different domains (a ''stripe-like'' and ''dot- like'') can coexist on the same terrace (Fig. 1a). They are separated by a line of white features that are 0.13 ± 0.02 nm high, 1.7 ± 0.1 nm wide and with lengths between 2.0 nm and 3.8 nm. The nature of this domain boundary is unknown. In atomically resolved STM images within a single domain only one elemental species is imaged (as in the insert of Fig. 2).

It is possible to reproduce the Moiré contrast with a model in which the sublattice of one kind of atoms in the *h*-BN layer is considered. A similar observation was made for the Moiré patterns created by NaCl adsorbed on Cu(1 1 1) [11] and on Al(1 0 0) [12], where only the Cl^- ions were imaged appearing as protrusions. Theoretical calculations for *h*-BN/Ni(1 1 1) show that the local density of states (LDOS) of N atoms around the Fermi level

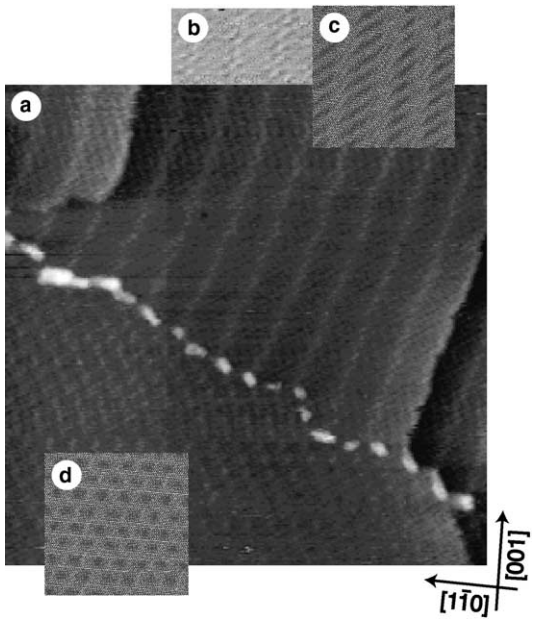

Fig. 1. (a) STM image ($V_s = 1$ V, $I = 1.0$ nA, 50×50 nm^2) of 1 ML *h*-BN/Pd(1 1 0). Two different Moiré patterns (a "stripe-like" and a "dot-like") separated by a domain boundary are shown. The upper "stripe-like" domain extends over three different terraces. (b) High-resolution STM image ($V_s = 1$ V, $I = 1.0$ nA, 15×8.5 nm^2) for a region of the stripe-like domain of (a). (c) and (d) Represent atomic models. The domain in (c) is produced by a clockwise rotation by 5° of a hexagonal layer of N atoms with respect to the [1 $\bar{1}$ 0] direction on the Pd(1 1 0) surface. The "dot-like" domain in (d) corresponds to the 0° orientation where one of the N–N Bravais vectors is aligned along [1 $\bar{1}$ 0].

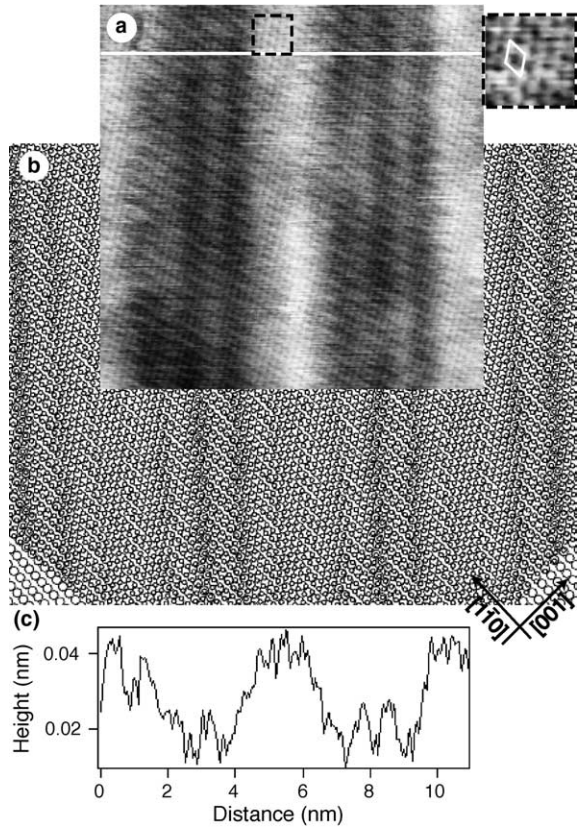

Fig. 2. (a) STM image ($V_s = -1$ V, $I = 2.0$ nA, 10×10 nm^2) of a single domain of 1 ML *h*-BN/Pd(1 1 0). This particular Moiré pattern is reproduced in an atomic model (b) with a counter-clockwise rotation of the N layer of 6° with respect to the [1 $\bar{1}$ 0] direction on Pd(1 1 0). The dashed square selection in (a) is enlarged in the insert (1×1 nm^2) on the right. It shows with atomic resolution the hexagonal layer and its unit cell. (c) Cross-sectional profile along the horizontal white line in (a).

is higher than the one of B [13]. Therefore it is likely that a corrugation within the N-superlattice generates the Moiré contrast in the *h*-BN/Pd(1 1 0) system. The Moiré patterns seen in the STM images are reproduced in a simple atomic model, where a hexagonal layer of N atoms is placed in certain orientations on a rectangular one, representing the Pd surface. In the top layer the N–N interatomic distance is 2.5 Å (as in bulk *h*-BN), while the Pd–Pd distance is 2.75 Å along the close-packed [1 $\bar{1}$ 0] direction and 3.89 Å along [0 0 1]. A 0° orientation defines the configuration in which one of the primitive lattice vectors of the hexagonal layer is parallel to the [1 $\bar{1}$ 0] crystallographic direction of the substrate. In a simple graphical overlay of these two layers, the darkest gray-scale value is produced whenever an N atom sits on top of a Pd atom. This procedure reproduces the observed STM contrast quite well, indicating that N-top sites have a higher tunneling resistance than bridge or hollow sites. The adsorption of a monolayer of C_{60} on top of the *h*-BN Moiré pattern inverts this contrast, reflecting the true topography of the layer (see below). The Moiré patterns are six-fold periodic: for a 60° rotation the same kind of pattern is found. For the 0° domain (see Fig. 1d) all these on-top positions form a hexagonal lattice with a lattice constant of 27.5 Å, which corresponds to 10 palladium or

11 nitrogen lattice constants along the [1 $\bar{1}$ 0] direction.

The "dot-like" pattern seen in the lower part of Fig. 1a is thus reproduced. The domain in the upper part of Fig. 1a can be simulated with a clockwise rotation of the overlayer by 5° with respect to the [1 $\bar{1}$ 0] direction of the substrate (Fig. 1c). The atomic model reproduces the Moiré pattern measured in a high-resolution image (Fig. 1b) in great detail, including the dark parallel lines that cross the bright stripes at a slanted angle. It appears that the microscope images bright ridges along the darker Moiré stripes (Fig. 1b), leading to the continuous bright stripes appearing in the STM image (Fig. 1a). Therefore, besides these topographic effects, also electronic effects seem to be present. They will not be studied in depth in this analysis since only the correct reproduction of the Moiré periodicity is searched.

A counterclockwise rotation of 6° (Fig. 2b) is needed to create the domain imaged in Fig. 2a. The line profile in Fig. 2c shows a small apparent corrugation of the Moiré contrast. This does not necessarily reflect the true topography of the overlayer, as was also discussed in the case of *h*-BN adsorbed on Rh(1 1 1) [5] and Ni(1 1 1) [10]. The insulating nature of *h*-BN in the tunneling window of these STM measurements (±2 V around the Fermi level) is the main cause for this phenomenon [13].

From the many STM images that were recorded in this study, it was not possible to identify the absolute predominance of one Moiré pattern with respect to the others. For a wide range of orientations (for example between 20° and 40° of rotation from the [1 $\bar{1}$ 0] direction) the contrast reproduced with atomic models is not very distinctive. Moreover the information obtained with the STM can represent only a small portion of the entire surface. The global information on the distribution of Moiré domains can be extracted from LEED experiments. LEED patterns recorded over a wide energy range (from 50 to 300 eV) show that a large circle surrounds each palladium principal lattice spot (Fig. 3a). Electron diffraction within the *h*-BN layer, which contains many rotated domains on this surface, creates this phenomenon. When the energy of the electrons is increased, the diame-

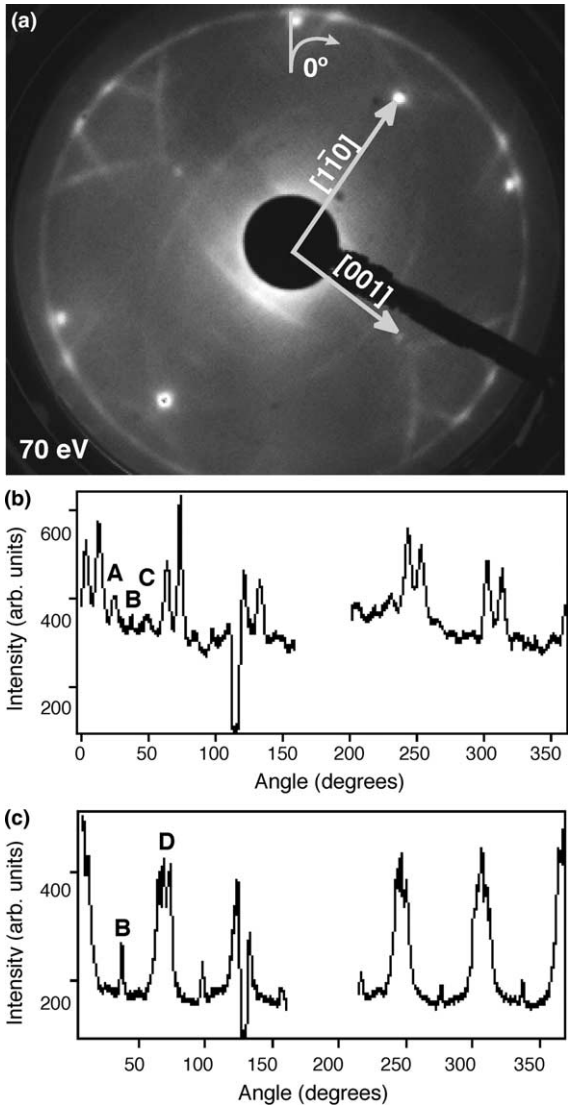

Fig. 3. (a) LEED image of 1 ML *h*-BN/Pd(1 1 0) recorded at 70 eV. A circle surrounds each Pd lattice spot. This is due to the electrons diffracted within the *h*-BN layer, which consists of several domains with different film orientations. In (b) the variation of the intensity along the circle centered at the (0,0) lattice spot is plotted. The zero azimuthal angle scale is given in the upper part of (a) and the angles are measured clockwise from there. The dominant twin-peaks occur at crossings with higher-order circles. In the region between 150° and 200° the circle is off limits of the image, at 115° the fixture of the electron gun is crossed. Peaks labeled "A"–"C" and "B" represent preferred domains (17° and 30°, respectively). (c) Shows the same kind of intensity profile for a different preparation, where the predominant domains, labeled "B"–"D" appear at 30° and 0°, respectively.

ter of the circle shrinks which is characteristic of simple in-plane scattering processes. From the radii of the circles a lattice constant of 2.51 ± 0.05 Å is determined, confirming that the circle represents an azimuthally smeared-out six-fold spot pattern due to the *h*-BN layer. Fig. 3a shows a typical LEED image measured at 70 eV, and Fig. 3b the distribution of the intensity along the circle centered at the (0,0) Pd lattice spot. The most intense peaks (twin-peaks) in the profile of Fig. 3b appear at the angles where the circle is crossed by other circles centered at some other Pd principal lattice spot. The minor peaks that show up in between contain information on domain abundances. Three series of peaks, each with a periodicity of 60°, can be found (the first one of each series is labeled A, B or C, respectively) corresponding to three preferred orientations of the *h*-BN layer. In the convention introduced for the STM images, series "B" corresponds to *h*-BN aligned with the [0 0 1] direction (30° orientation), series "A" and "C" to a counterclockwise and a clockwise rotation of $17.0° \pm 0.5°$, respectively.

The profile in Fig. 3c belongs to a LEED image recorded at the same energy in a different experiment. It reflects a dramatically different domain distribution: besides the intense twin-peaks only two series of peaks clearly stand out, labeled "D" and "B". The peaks "D" appear in the center of the twin-peaks and correspond to *h*-BN oriented along the $[1\bar{1}0]$ direction (0° orientation). The peaks "B" correspond again to *h*-BN aligned along the [0 0 1] direction (30° orientation) as in the previous profile (Fig. 3b). The Moiré pattern that would correspond to this latter configuration is not distinctive. The coincidence of N on top positions should appear every nine palladium lattice constants or every 14th nitrogen atom along [0 0 1].

The reason for the different domain distribution formed in this case is not clear; it might be attributed to the different procedure used to clean the Pd sample. After the cycles of sputtering in the case of the first profile (Fig. 3b) the sample was exposed to 8 L of O_2, while in the second case (Fig. 3c) 45 L of O_2 have been used. The exposure to high doses of oxygen is known to be efficient for removing carbon contaminants. Another possible reason might be the slightly contaminated $(HBNH)_3$ precursors used in the second case. In the analysis of several LEED profiles (as those of Fig. 3b and c) obtained from images recorded at different energies and for different but equivalent sample preparations, the domain with 30° orientation (peak "B") has always been found. Therefore this configuration is one of the energetically most stable ones. The other domains do not always appear predominantly. To test the thermal stability of the Moiré structures in general, the sample was annealed under the LEED apparatus. The ring shows up to at least 950 K and the domain distribution along it does not change significantly.

The last part of this experimental study addresses the preparation and analysis of C_{60} monolayers adsorbed on these nanostructured Moiré domains. Besides the principal Pd spots, the LEED patterns do not show extra spots due to the C_{60} adlayer; the *h*-BN ring is strongly suppressed and only the twin-peaks (as in Fig. 3b) are still visible. Nevertheless the STM images (Fig. 4a and c) show highly regular domains that are interpreted as C_{60} Moiré patterns on top of *h*-BN Moiré patterns. In the model depicted in Fig. 4b the *h*-BN layer is rotated counterclockwise by 1° with respect to the substrate (a domain similar to the "dot-like" of Fig. 1a), and in Fig. 4d there is a 5° counterclockwise rotation. A distance of 10 Å between the C_{60} molecules has been used in the model, since an average value of 9.7 ± 0.7 Å has been determined from several STM images. The brightest C_{60} molecules in the STM images correspond, in the model, to molecules covering an area with a high density of N atoms placed on top or nearly on top of Pd atoms. The Moiré contrast is mainly defined by the orientation of the *h*-BN layer while the C_{60} molecules accommodate themselves in order to follow the topography below. Since the C_{60} molecules form a conducting overlayer, it is possible to estimate a corrugation of the Moiré pattern from STM line profiles (as Fig. 4e). The differences in height between the brightest and darkest C_{60} molecules yield a value of 0.53 ± 0.12 Å as determined from the analysis of different images recorded at tunneling voltages between 1 V and 2 V. Moreover, by means of LEED and STM it has been demon-

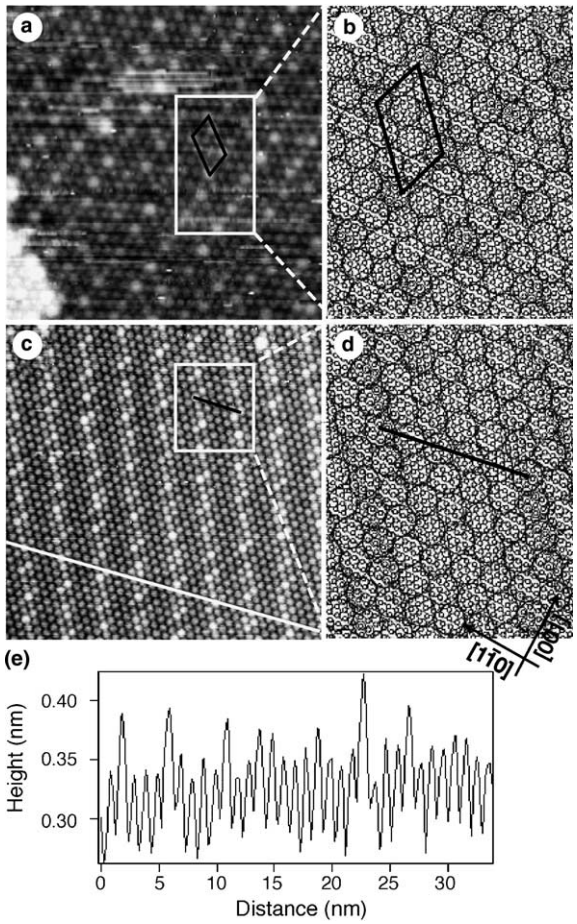

Fig. 4. (a) and (c) STM images ((a) $V_s = 2$ V, $I = 1$ nA, 23×23 nm^2; (c) $V_s = 1$ V, $I = 2$ nA, 30×30 nm^2) of 1 ML of C_{60} on 1 ML *h*-BN/Pd(1 1 0). The brightness contrast in these two coexisting domains is interpreted as a C_{60} layer following the configuration of the *h*-BN Moiré pattern. In a microscopic model ((b) and (d)) the global Moiré contrast is mainly defined by the orientation of the *h*-BN layer. Thus the bright molecules appear as dark spots since they correspond to C_{60} covering areas with a high density of N atoms on top or nearly on top of Pd atoms (darkest regions). (b) and (d) Reproduce atomically the rectangular areas of (a) and (b), respectively. While in (a) the *h*-BN layer is rotated by 1° counterclockwise away from the [1 $\bar{1}$ 0] crystallographic direction of the substrate, in (c) the layer is rotated of 5° counterclockwise. Black lines follow periodic features of the patterns. (e) Cross-sectional profile along the diagonal continuous white line in (c).

strated that nanostructures formed in 1 ML *h*-BN/Pd(1 1 0), and 1 ML of C_{60} adsorbed on it, are stable even after air exposure.

4. Conclusions

In conclusion we have characterized the complex morphology of *h*-BN grown on the Pd(1 1 0) surface. Due to the different lattice constant and symmetry of overlayer and substrate, the system forms *h*-BN domains with quasi-random orientations. STM images show several Moiré patterns where the contrast is due to nitrogen adatoms occupying different adsorption sites on the Pd(1 1 0) surface. A topographic corrugation of this layer of 0.5 Å can be estimated. The resulting Moiré patterns and corrugation persist when C_{60} molecules are adsorbed to form a monolayer. From the analysis of LEED images we learn that the alignment along the [0 0 1] crystallographic direction is one of the preferred orientations. We provide indications that this system may be a model example of a "tunable nanostructure". The exposure to specific doses of H_2, for example, might lead to the disappearance of some domains at the expense of the most favored ones. Moreover the choice of a particular Pd(1 1 0) vicinal surface might give the possibility to grow films with a single Moiré domain and thus with a single monoperiodicity and symmetry. The potential utility of this system is even enhanced when C_{60} layers are grown on top of the *h*-BN film. The C_{60} molecules "memorize the substrate corrugation", following the topographic patterns generated by the underlying *h*-BN film.

Acknowledgement

We thank J. Barth for the loan of the Pd(1 1 0) sample, H. Sachdev for the production of borazine and M. Klöckner for technical assistance. This project is supported by the Swiss National Science Foundation.

References

[1] J.-W. He, D.W. Goodman, Surf. Sci. 232 (1990) 138.
[2] M.T. Paffett, R.J. Simonson, P. Papin, R.T. Paine, Surf. Sci. 232 (1990) 286.

[3] A. Nagashima, N. Tejima, Y. Gamou, T. Kawai, C. Oshima, Surf. Sci. 357–358 (1996) 307.
[4] A. Nagashima, N. Tejima, Y. Gamou, T. Kawai, C. Oshima, Phys. Rev. Lett. 75 (1995) 3918.
[5] M. Corso, W. Auwärter, M. Muntwiler, A. Tamai, T. Greber, J. Osterwalder, Science. 303 (2004) 217.
[6] R.M. Desrosiers, D.W. Greve, A.J. Gellman, Surf. Sci. 382 (1997) 35.
[7] A. Nagashima, N. Tejima, Y. Gamou, T. Kawai, M. Terai, C. Oshima, Phys. Rev. B 51 (1995) 4606.
[8] W. Auwärter, T.J. Kreutz, T. Greber, Surf. Sci. 429 (1999) 229.
[9] W. Auwärter, M. Muntwiler, T. Greber, J. Osterwalder, Surf. Sci. 511 (2002) 379.
[10] W. Auwärter, One monolayer of Hexagonal Boron Nitride on Ni(111): an atomically sharp interface, Ph.D. Thesis, University of Zürich, 2003.
[11] J. Repp, G. Meyer, K.-H. Rieder, Phys. Rev. Lett. 92 (2004) 036803.
[12] W. Hebenstreit, J. Redinger, Z. Horozova, M. Schmid, R. Podloucky, P. Varga, Surf. Sci. 424 (1999) L321.
[13] G.B. Grad, P. Blaha, K. Schwarz, W. Auwärter, T. Greber, Phys. Rev. B 68 (2003) 085404.